

## THE ANISOTROPIC YOUNG'S MODULUS OF EQUINE SECONDARY OSTEONES AND INTERSTITIAL BONE DETERMINED BY NANOINDENTATION

JAE-YOUNG RHO<sup>1</sup>, JOHN D. CURREY<sup>2,\*</sup>, PETER ZIOUPOS<sup>3</sup> AND GEORGE M. PHARR<sup>4</sup>

<sup>1</sup>Department of Biomedical Engineering, University of Memphis, Memphis, TN 38152, USA, <sup>2</sup>Department of Biology, University of York, PO Box 373, York YO10 5YW, UK, <sup>3</sup>Department of Materials and Medical Sciences, Cranfield University, Shrivenham SN6 8LA, UK and <sup>4</sup>Department of Material Sciences, University of Tennessee, Knoxville, TN 37996, USA and Metals and Ceramics Division, Oak Ridge National Laboratory, Oak Ridge, TN 37831, USA

\*Author for correspondence (e-mail: jdc1@york.ac.uk)

Accepted 27 February; published on WWW 23 April 2001

### Summary

The equine radius is a useful subject for examining the adaptation of bone histology to loading because in life the anterior cortex is loaded almost entirely in tension, the posterior cortex in compression. The histology of the two cortices is correspondingly different, the osteones and the interstitial lamellae in the posterior cortex having a more transversely oriented fibre arrangement than those in the anterior cortex. Presumably as a result of this histological difference, the posterior cortex is stronger in compression than the anterior cortex; the anterior cortex is stronger in tension than the posterior cortex. We here use nanoindentation to examine how the Young's modulus of elasticity of secondary osteones and interstitial lamellae in the anterior and posterior cortices varied as a function of angle.

The anterior osteones were stiffer than the posterior osteones when tested in the direction parallel to the bone's long axis, but became progressively relatively less stiff as the angle increased; at 90°, they were less stiff than the posterior osteones. Although the interstitial lamellae were stiffer than their neighbouring osteones, the same relationship between anterior and posterior interstitial lamellae as a function of angle was found as for the osteones. The anisotropy of these Young's moduli determined by nanoindentation shows a close relationship with what was to be expected from the histological findings.

Key words: bone, Young's modulus, anisotropy, nanoindentation, osteone, horse, *Equus caballus*.

### Introduction

It is generally regarded almost as a truism that the architectures of bones are adapted to their mechanical environment. However, bones in which the internal histological structure can be shown to be so adapted are much rarer. This is mainly because it is difficult to quantify the stresses acting in a bone. Furthermore, if these stresses vary over time, it is difficult to be sure what the histology may be adapting to. The radius of the horse is important for understanding histological adaptation because its loading system is so simple. The bone has a gentle anterior curvature. This curvature interacts with longitudinal forces imposed during locomotion to produce bending, so that the anterior cortex is loaded in tension and the posterior cortex is loaded in compression (Rubin and Lanyon, 1982; Biewener et al., 1983a; Biewener et al., 1983b).

Riggs et al. (Riggs et al., 1993a; Riggs et al., 1993b) showed that this loading pattern is associated with differences in histology. The anterior (cranial) cortex characteristically remodels rather little, and the secondary osteones (called hereafter simply osteones) that form have a predominantly longitudinal orientation of their mineral and collagen. The

posterior (caudal) cortex remodels considerably, and the osteones so formed have a more transverse orientation of the mineral and collagen (Riggs et al., 1993a; Mason et al., 1995; Batson et al., 2000). This difference in the arrangement of the tissue was confirmed by Fratzl et al. (Fratzl et al., 1996) using small-angle X-ray scattering. They could not, using that method, distinguish between crystals in the osteones and those in the interstitial lamellae, and at all sites there were crystals oriented in all directions. Nevertheless, they could show that the anterior cortex had a much larger number of crystals orientated at a very small angle to the long axis than did the posterior cortex. The osteones from the posterior cortex were, viewed along the length of the bone in polarised light microscopy, generally bright from their periphery to the central lumen, though often showing alternating lamellae that were bright and dark. Osteones from the anterior cortex were usually dark for most of their area. Quite often, however, there was a peripheral bright ring. These differences in brightness are produced by the form birefringence of bone. When the grain of the bone is orientated towards the observer, the bone appears relatively dark; when the grain is at an angle to the viewer, the

bone appears relatively light. Unfortunately, it is difficult to quantify the relationship between differences in brightness and the grain of the bone (Carando et al., 1991). The implication of these findings is that the grain of the osteons in the anterior (tension) cortex is more longitudinally oriented with respect to the long axis of the bone than it is in the posterior (compression) cortex.

These structural differences in the two cortices are in turn associated with differences in mechanical properties (Riggs et al., 1993b). In particular, in quasi-static loading, the anterior bone had a higher Young's modulus than the posterior bone whether loaded in tension or in compression; the anterior bone was stronger in tension than the posterior bone, while the posterior cortical bone was stronger in compression than the anterior bone. Schryver (Schryver, 1978), Reilly and Currey (Reilly and Currey, 1999) and Batson et al. (Batson et al., 2000) showed that specimens from the anterior cortex were also stiffer and stronger in bending. Furthermore, Batson et al. (Batson et al., 2000) showed that the anterior cortex was much stronger in bending impact than the posterior cortex (Table 1).

That these characteristically different types of osteons from the anterior and posterior cortices seem to be adapted to different loading regimes, are significant constituents of bony tissues that have different strengths in tension and in compression and have different histological structures, makes them ideal candidates for examining the relationships between mechanical properties and histology. Until recently, the mechanical properties of bone have been examined on machined specimens, which inevitably have sizes of the order of millimetres and, often, much more. However, bone has a hierarchical structure, and the size of relatively large specimens hides the different contributions of elements lower down in the hierarchy. With the advent of nanoindentation and the ability to determine the elastic modulus from the known load *versus* depth-of-deformation behaviour of the nanoindenter (Oliver and Pharr, 1992), it is becoming possible to analyse the elastic behaviour of bone at a rather low level in the hierarchy (e.g. Hoffler et al., 2000; Rho et al., 1997; Rho et al., 1999a; Rho et al., 1999b). Here, we describe the use of nanoindentation to explore the anisotropic elastic behaviour of bone of different histological types

and show how differences in behaviour are related to the orientation of loading.

Ziv et al. (Ziv et al., 1996) found, using microindentation, that 'Microhardness measurements made face-on to the layers of crystals and collagen triple helical molecules, show much lower values than those made edge-on to these layers.' Because hardness and Young's modulus are well-correlated (Rho et al., 1999a), it is to be expected that nanoindentation measurements would show the same trends.

What we set out to do in this work, and what we believe is novel, is to examine, using nanoindentation, the moduli of elasticity both of osteons and of interstitial lamellae as a function of angle with respect to the long axis of the bone. Furthermore, we carried out this work on the radius of the horse, which is known to have a different predominant orientation of the grain of the bone in the anterior and posterior cortices and would, therefore, be expected to show different degrees of anisotropy. Our results confirm these expectations and give new information about how bony tissues with different histological anisotropies show different mechanical anisotropies.

### Materials and methods

Specimens were prepared from the mid-shaft of the radius of a 2-year-old Thoroughbred horse *Equus caballus* L. Eight rectangular parallelepiped specimens, approximately 5 mm×5 mm×10 mm, were obtained from the anterior and posterior cortex, from regions that had undergone considerable reconstruction. (Unusually, the anterior cortex was considerably remodelled, allowing us to sample easily osteons subjected to tensile loading.) From these specimens, blocks were prepared that had one face at 0°, 15°, 45° or 90° to the bone's transverse plane, the slope being in the radial direction. An undecalcified section, approximately 100 µm thick, was prepared from the bone adjacent and parallel to these surfaces for examination by polarised light microscopy.

Each block was dehydrated in a series of alcohol baths and embedded without vacuum in epoxy resin at room temperature (20 °C; EPO-THIN low-viscosity epoxy, Buehler, Lake Bluff, IL, USA). The embedded specimen was

Table 1. Mean values of the mechanical properties of bone material from the anterior and posterior cortices of the equine radius

| Load in life: | Young's modulus (GPa) |           | Static strength (MPa) |           | Impact strength (kJ m <sup>-2</sup> ) |           | Reference               |
|---------------|-----------------------|-----------|-----------------------|-----------|---------------------------------------|-----------|-------------------------|
|               | Ant Tens              | Post Comp | Ant Tens              | Post Comp | Ant Tens                              | Post Comp |                         |
| Load in test  |                       |           |                       |           |                                       |           |                         |
| Tension       | 22.1                  | 15.0      | 161                   | 105       | –                                     | –         | Riggs et al., 1993b     |
| Compression   | 18.6                  | 15.3      | 185                   | 217       | –                                     | –         | Riggs et al., 1993b     |
| Bending       | 20.1                  | 16.2      | 249                   | 217       | –                                     | –         | Schryver, 1978          |
| Bending       | 21.1                  | 15.5      | 232                   | 203       | –                                     | –         | Reilly and Currey, 1999 |
| Bending       | 17.9                  | 13.5      | 201                   | 154       | 32.6                                  | 17.5      | Batson et al., 2000     |

Ant, anterior cortex; Post, posterior cortex; Tens, tension in life; Comp, compression in life.

polished metallographically to produce the smooth surfaces needed for nanoindentation testing: after being ground using silicon carbide abrasive papers of decreasing grit size (600, 800 and 1200 grit) under deionized water, the specimens were polished on microcloths with successively finer grades of alumina powder, the finest being 0.05  $\mu\text{m}$  grit; the last polishing step was on plain microcloth under deionized water, and the specimen was cleaned ultrasonically to remove surface debris.

All nanoindentation tests (Nano Indenter II, MTS Systems Co., Oak Ridge, TN, USA) were conducted in load control. The specimens were loaded dry. The position of each indentation was selected manually. Each nanoindentation test used a maximum load of 4 mN, which produces hardness impressions with depths of approximately 600 nm. The hardness and elastic modulus for each indentation were determined, using the method of Oliver and Pharr, from the first 50% of the unloading curves, the data being obtained in the third unloading segment (Oliver and Pharr, 1992; Rho et al., 1997; Rho et al., 1999a; Rho et al., 1999b). Fused silica, which is elastically isotropic and which has a relatively low modulus-to-hardness ratio, was used to calibrate the tip shape function and to check on the accuracy of the measurements. The elastic modulus measured for the fused silica,  $72.1 \pm 0.5$  GPa (mean  $\pm$  s.d.,  $N=60$ ), was essentially the same as the canonical value, 72.0 GPa.

Indentations were made on anterior and posterior cortices, on osteones and on interstitial bone, at four different angles on 16 different fields; 4–12 indentations were made for each field. It was simple to distinguish osteones from interstitial bone except when the indentation direction was at  $90^\circ$  to the long axis of the bone; at this angle, the histology did not show the characteristic shape of osteones. These  $90^\circ$  sites were considered to be osteones if they were less than 50  $\mu\text{m}$  from a Haversian canal. Nevertheless, attributions to interstitial bone at  $90^\circ$  were somewhat problematical because, although there was not much doubt about the attribution to an osteone if a Haversian canal was visible, 'interstitial' indentations might have been made within osteones whose canal was out of the plane of the section. Despite this, as we shall see, what we considered to be interstitial bone at  $90^\circ$  had markedly different properties from the osteonal bone. We could not determine the long axis of individual osteones but, because most osteones run roughly parallel to the long axis of the bone, indentation angle with respect to the bone axis is a good indication of angle with respect to the osteone.

Most osteones, when seen under polarised light in sections taken normal to the long axis of the bone, have a peripheral layer of highly birefringent bone, indicating that there the predominant grain of the bone structure is at a large, although unknown, angle to the long axis of the bone. Accordingly, we selected fields within the osteones approximately half-way between the edge of the canal and the cement line bounding the osteone, not close to this peripheral layer. To examine the mechanical properties of this peripheral layer further, we tested six osteones from the anterior and five from the

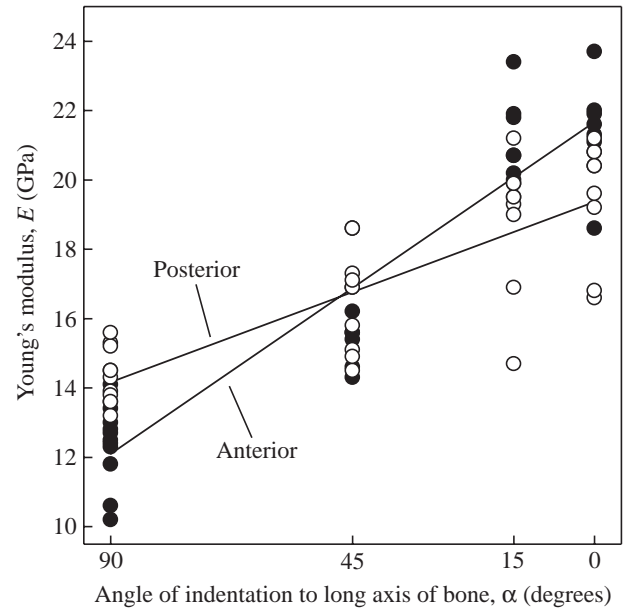


Fig. 1. The relationship between the angle of the indentation direction to the long axis of the bone ( $\alpha$ ; degrees) and Young's modulus ( $E$ ; GPa) for osteones. Note that the ordinate does not start at zero. Open circles, osteones from the posterior cortex; filled circles, specimens from the anterior cortex. The sloping thick lines are the regression lines of  $E=a+b\alpha$  from Table 2.

posterior cortex at  $0^\circ$ . In each osteone, we took one measurement half-way along the radius joining the central canal to the periphery ('mid') and one measurement close to the periphery ('outer').

## Results

Fig. 1 shows the Young's modulus of osteones from anterior and posterior cortices at various angles to the long axis of the bone. Table 2 gives the linear regressions describing the relationships. (We used the linear regression model because it is the simplest; we had no particular *a priori* model.) Compared with osteones from the posterior cortex, osteones from the

Table 2. Linear regressions describing the relationship between the Young's modulus ( $E$ ) of the osteones or interstitial lamellae and the angle  $\alpha$  the direction of indenting makes to the long axis of the bone

| Source                 | $N$ | $a$  | $b$    | $t$  | $r^2$ |
|------------------------|-----|------|--------|------|-------|
| Anterior osteones      | 35  | 21.7 | -0.106 | 15.8 | 0.88  |
| Posterior osteones     | 35  | 19.4 | -0.058 | 8.2  | 0.66  |
| Anterior interstitial  | 24  | 23.8 | -0.117 | 28.9 | 0.97  |
| Posterior interstitial | 24  | 22.1 | -0.079 | 15.8 | 0.92  |

$N$ , sample size;  $a$ ,  $b$ , coefficients in the equation  $E=a+b\alpha$ .

Young's modulus  $E$  is in GPa; angle  $\alpha$  is in degrees.

$r^2$  is calculated allowing for degrees of freedom.

All coefficients were significant at  $P<0.001$ .

Table 3. Results of an analysis of covariance for various comparisons

| Comparison                              | Null hypothesis | F (d.f.)      | P       |
|---|-----------------|---------------|---------|
| Anterior versus posterior osteones      | Slopes same     | 11.03 (1,67)  | <0.001  |
|   | Heights same    | —             | —       |
| Anterior versus posterior interstitial  | Slopes same     | 35.75 (1,45)  | <0.001  |
|   | Heights same    | —             | —       |
| Anterior, osteones versus interstitial  | Slopes same     | 1.56 (1,56)   | NS      |
|   | Heights same    | 24.17 (1,55)  | <0.001  |
| Posterior, osteones versus interstitial | Slopes same     | 5.01 (1,56)   | <0.05   |
|   | Heights same    | 24.11 (1,55)* | <0.001* |

\*Note that if the null hypothesis that the slopes are the same is rejected, then the null hypothesis that the heights are the same has no universal meaning because the regression lines must intersect somewhere. However, in the case of posterior osteones versus interstitial lamellae, which is significant at  $P < 0.05$ , inspection of Fig. 3 shows that, over the total range of angles possible, the two lines are separate, and the analysis of covariance suggests that the heights are clearly different.

NS, not significant.

anterior cortex are stiffer when the loading is parallel to the long axis ( $0^\circ$ ) but less stiff when the loading is normal to the long axis ( $90^\circ$ ). The anisotropy in stiffness of the anterior cortical osteones is considerable, Young's modulus ranging from a mean of 12.4 GPa to 21.4 GPa. The range for the posterior cortical osteones was smaller, from 14.5 to 19.4 GPa.

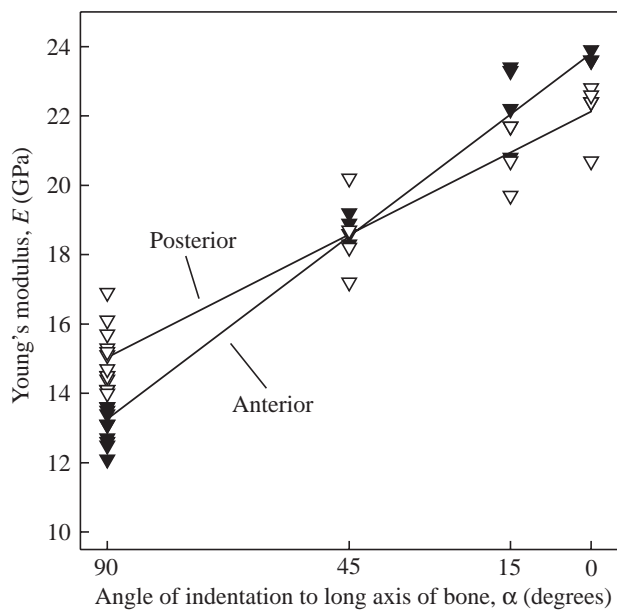


Fig. 2. The relationship between the angle of the indentation direction to the long axis of the bone ( $\alpha$ ; degrees) and Young's modulus ( $E$ ; GPa) for interstitial lamellae. Open triangles, posterior interstitial lamellae; filled triangles, anterior interstitial lamellae. The sloping lines are the regression lines (see Table 2 for regression coefficients).

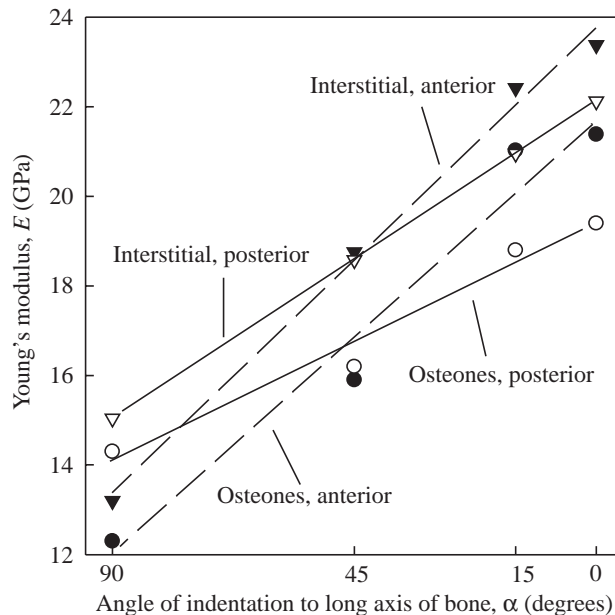


Fig. 3. Regression lines for all four types of specimen. The symbols refer to the mean values at each angle. Open circles, posterior osteones; filled circles, anterior osteones; open triangles, posterior interstitial lamellae; filled triangles, anterior interstitial lamellae; dashed lines, anterior specimens; continuous lines, posterior specimens.

Both slopes are highly significantly different from zero, and the differences between the slopes are themselves highly significant (Tables 2, 3). That is to say, the anterior osteones are more anisotropic in their Young's modulus than are the posterior osteones.

Fig. 2 and Tables 2 and 3 show the corresponding pattern and regression equations for the interstitial bone taken adjacent to the osteones. Again, there is a decrease of modulus with angle, and the distributions cross each other, with the anterior specimens being less stiff than the osteonal specimens at  $90^\circ$  but stiffer at  $0^\circ$ . Furthermore, the anterior specimens are again more anisotropic than the posterior ones.

Fig. 3 shows the mean values for the different types of specimens at various angles and their regression lines. The reduction in clutter allows osteones and interstitial regressions to be compared visually. The lines for anterior specimens (osteones or interstitial, dashed) are roughly parallel, the exponents for slope, as shown in Table 2, being similar; the lines for the posterior specimens (continuous) are somewhat less parallel. At angles less than  $90^\circ$ , the interstitial specimens are stiffer than the osteonal specimens, and the interstitial specimens are always stiffer than their corresponding osteonal specimens, even at  $90^\circ$ .

Fig. 4 shows the stiffness of lamellae from the 11 osteones tested, at  $0^\circ$ , in two wall positions: mid and outer. Tables 4–6 give the analyses of the results for these specimens. In osteones from both cortices, the mid layer is stiffer than the outer layer and, as would be expected, the posterior cortical osteones are generally less stiff than the anterior cortical osteones.

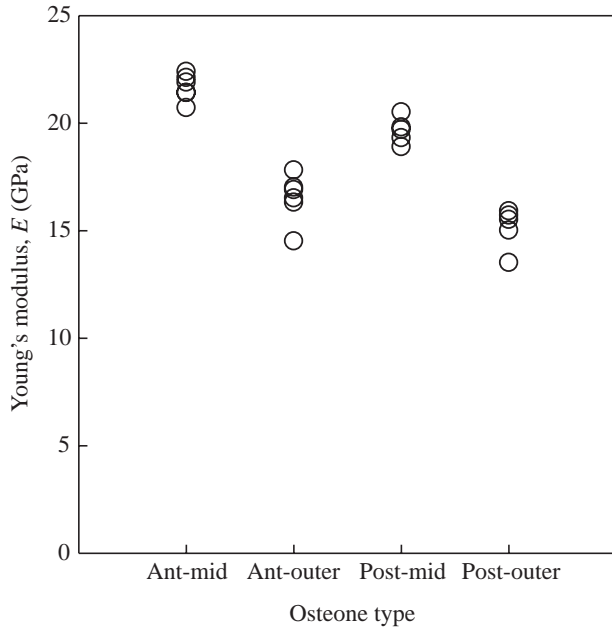


Fig. 4. Young's moduli for anterior and posterior osteones tested in the middle of the wall and in the outer region. Some points have been displaced slightly (by up to 0.2 GPa) to make all the circles visible. Ant-mid, anterior osteone, middle; Ant-outer, anterior osteone, outer; Post-mid, posterior osteone, middle; Post-outer, posterior osteone, outer.

**Discussion**

First, we should point out that we have used samples from only one bone and, therefore, we have no idea of the variability that may be found between different bones. There is, of course, some variability between the values found within sites, but not so much as to obscure the extremely statistically significant differences between sites. The results agree in the ways that could be measured with those from larger data sets (the general histology of the bones, the difference in the Young's modulus when measured in the longitudinal direction between the anterior and posterior cortex, and the difference in modulus, determined by nanoindentation, between the bone within the osteones and the interstitial lamellae), so there is no reason for thinking that the bone we used was exceptional in any way.

Consider Fig. 1 first. Both anterior and posterior osteones show an increase in Young's modulus as the direction of indentation becomes more aligned with the long axis of the

Table 4. Mean values of the Young's modulus of the two types of osteone loaded in two different places, mid and outer

| Osteone type     | N | Young's modulus (GPa) |
|------------------|---|-----------------------|
| Anterior, mid    | 6 | 21.65±0.59            |
| Anterior, outer  | 6 | 16.48±1.08            |
| Posterior, mid   | 5 | 19.64±0.58            |
| Posterior, outer | 5 | 15.12±0.96            |

Values are means ± S.D.

Table 5. Results of an analysis of variance of the two types of osteone loaded in two different places

| Source       | d.f. | SS    | MS   | F    | P      |
|--------------|------|-------|------|------|--------|
| Osteone type | 3    | 146.7 | 48.9 | 70.5 | <0.001 |
| Error        | 18   | 12.6  | 0.70 |      |        |
| Total        | 21   | 159.2 |      |      |        |

There is highly significant overall heterogeneity.  
d.f., degrees of freedom; SS, sum of squares; MS, mean square.

bone. The grain of the bone is predominantly longitudinal, so the bone will be stiffest when the indentation is at 0°. Furthermore, the anterior osteones are stiffer than the posterior osteones at 0° and less stiff at 90°. This is again to be expected because the anterior osteones, being adapted to tension, have fibres running in a more longitudinal direction than the posterior osteones (Riggs et al., 1993a). On average, the fibres in the anterior osteones will be loaded more fully end-on at 0° and more fully side-on at 90° than the posterior osteones and will, therefore, show a greater anisotropy. These results accord with our expectations derived from histology.

The interstitial lamellae behave in roughly the same way as the osteones (Fig. 2). They are generally stiffer than the osteones (Fig. 3), except at 90°, where the anterior interstitial lamellae are less stiff than the posterior osteones. The 0° results agree with previous findings (Rho et al., 1999a; Rho et al., 1999b); interstitial lamellae are in general stiffer than osteonal lamellae. This is presumably because they are older and have had more time in which become fully mineralised.

Ziv et al. (Ziv et al., 1996), using microindentation rather than nanoindentation on bovine femora and rat tibiae, showed that there were variations in Vickers hardness number (not Young's modulus, which cannot be determined using microhardness) with orientation. Because all the bone they examined was primary, they did not, of course, relate these differences to osteones and interstitial lamellae.

Compared with the osteone results, the differences between the anterior and posterior interstitial lamellae are less secure because it is unclear what proportion of these interstitial

Table 6. Fisher's pairwise comparison of the Young's moduli for all possible combinations of the osteones loaded in two different places

|                  | Anterior, mid | Anterior, outer | Posterior, mid |
|------------------|---------------|-----------------|----------------|
| Anterior, outer  | 3.78 to 6.55  |                 |                |
| Posterior, mid   | 0.55 to 3.47  | -4.61 to -1.70  |                |
| Posterior, outer | 5.07 to 7.99  | -0.09 to 2.82   | 3.00 to 6.04   |

Individual rate is set at 0.01.

The numbers are the confidence intervals for the values of column mean to row mean.

The table indicates that the only difference that is not significant is anterior outer versus posterior outer (this is the only comparison for which the confidence intervals include zero).

lamellae is primary and what proportion is secondary. Osteones (which is what we have called secondary osteones in this paper) are, by definition, secondary and are therefore necessarily younger than the surrounding bone. Interstitial lamellae may be remnants of osteones, or may be remnants of primary lamellar bone or, possibly in the case of the horse, of primary fibrolamellar bone (Francillon-Vieillot et al., 1990). However, when remodelling is intense, as had been the case in the specimens examined here, most of the interstitial bone is probably itself secondary, although almost certainly some will not be.

Insofar as the interstitial bone consists of remnants of secondary bone, the results we have obtained are as expected; the interstitial bone behaves like its neighbouring osteones, but is on average stiffer because it is older and more highly mineralised. There is no evidence for or against the possibility that the primary fibrolamellar bone, which is the first bone to be laid down in the long bones of the horse, is different in the anterior and posterior cortices of the horse radius. If substantial amounts of the interstitial bone had been the remnants of fibrolamellar bone, and if this bone were the same in the anterior and posterior cortices, one would have expected the anterior and posterior interstitial bone tissues to be more similar than they in fact are. The observation that the interstitial bone behaves very similarly to the osteonal bone suggests either that the primary bone in the two cortices is dissimilar or, more probably, that the interstitial bone is usually the remnants of osteones.

The results of indentations on anterior and posterior osteones in two places within the osteones (Fig. 4) are less satisfactory. The anterior osteones are predominantly dark, but usually with a bright ring at the periphery (Riggs et al., 1993a; Batson et al., 2000). The posterior osteones are much more uniformly bright. We had hypothesised that the large difference in orientation between different parts of the anterior osteones, suggested by the bright ring, would result in there being a greater difference between 'anterior-mid' and 'anterior-outer' than between 'posterior-mid' and 'posterior-outer'. Although the mean difference is indeed greater (5.2 GPa and 4.5 GPa respectively; see Table 4), Table 6 shows, not surprisingly, that the difference does not even approach significance. However, it has been shown (Rho et al., 1999b) that the outer parts of 'ordinary' osteones, from the middle of the cortex of the human femur, are less stiff than the more central parts, probably because they are less highly mineralised, and so this particular phenomenon may simply be part of what is found in all osteones and nothing to do with the two sets of osteones described in this paper being adapted to different loading. Furthermore, if the bright ring were caused by there being a low proportion of longitudinally oriented bone in it, one would expect the stiffness to be similar to the stiffness of anterior osteones when loaded at 90°. In fact, the stiffness of the bright-ring specimens is greater than this (Figs 3, 4). It is possible, because we could not exactly match polarised light images to our indentation sites, that we did not sample in all cases in the ring itself.

The bone of the anterior and posterior cortices of the equine radius, which is subjected to different loading modes, has Young's moduli, determined by nanoindentation, that agree with what is to be expected from the histology of the bone in these cortices. In particular, the variation in Young's modulus with the degree of off-axis loading accords well with the more longitudinal orientation of the bone in the anterior cortex as opposed to the posterior cortex. These differences in behaviour are found in both the osteones and the interstitial bone.

We have demonstrated here the value of nanoindentation estimates of Young's modulus in gaining a clearer understanding of the variation in the stiffness of bone throughout bony tissue, and at different orientations, and the relationship between this variation and the bone's histological structure. We have added to the understanding of the relationship between the loading, histology and mechanical properties of bone in a very valuable model system, the horse's radius.

The nanoindentation work was sponsored in part by NIH AR45297 and NSF DMR-0076497. Instrumentation for the nanoindentation work at the Oak Ridge National Laboratory SHaRE User Facility was provided by the Division of Materials Sciences and Engineering, US Department of Energy, under Contract DE-AC05-96OR22464 with Lockheed Martin Energy Corp. and through the SHaRE Program under Contract DE-AC05-00OR22725 with UT-Battelle, LLC and through the SHaRE Program under Contract DE-AC05-76OR00033 with Oak Ridge Associated Universities. P.Z. acknowledges the support of the EPSRC (GR/M59167, GR/N33225). We are thankful to Professor Allen Goodship for providing the horse radius and to anonymous referees for helpful comments.

## References

- Batson, E. L., Reilly, G. C., Currey, J. D. and Balderson, D. S. (2000). Post-exercise and positional variation in mechanical properties of the radius in young horses. *Equine Vet. J.* **32**, 95–100.
- Biewener, A. A., Thomason, J., Goodship, A. and Lanyon, L. E. (1983a). Bone stress in the horse forelimb during locomotion at different gaits: a comparison of two experimental methods. *J. Biomech.* **16**, 565–576.
- Biewener, A. A., Thomason, J. and Lanyon, L. E. (1983b). Mechanics of locomotion and jumping in the forelimb of the horse (*Equus*): *in vivo* stress developed in the radius and metacarpus. *J. Zool., Lond.* **201**, 67–82.
- Carando, S., Portigliattibarbos, M., Ascenzi, A., Riggs, C. M. and Boyde, A. (1991). Macroscopic shape of and lamellar distribution within, the upper limb shafts, allowing inferences about mechanical-properties. *Bone* **12**, 265–269.
- Francillon-Vieillot, H., de Buffrénil, V., Castanet, J., Géraudie, J., Meunier, F. J., Sire, J. Y., Zylberberg, L. and de Ricqlès, A. (1990). Microstructure and mineralization of vertebrate skeletal tissues. In *Skeletal Biomineralization: Patterns, Processes and Evolutionary Trends*, vol. 1 (ed. J. G. Carter), pp. 471–530. New York: Van Nostrand Reinhold.
- Fratzl, P., Schreiber, S. and Boyde, A. (1996). Characterization of bone mineral crystals in horse radius by small angle X-ray scattering. *Calcif. Tissue Int.* **58**, 341–346.
- Hoffler, C. E., Moore, K. E., Kozloff, K., Zysset, P. K., Brown, M. B. and Goldstein, S. A. (2000). Heterogeneity of bone lamellar-level elastic moduli. *Bone* **26**, 603–609.

- Mason, M. W., Skedros, J. G. and Bloebaum, R. D.** (1995). Evidence of strain-mode-related cortical adaptation in the diaphysis of the horse radius. *Bone* **17**, 229–237.
- Oliver, W. C. and Pharr, G. M.** (1992). An improved technique for determining hardness and elastic modulus using load and displacement sensing indentation experiments. *J. Mater. Res.* **7**, 1564–1583.
- Reilly, G. C. and Currey, J. D.** (1999). The development of microcracking and failure in bone depends on the loading mode to which it is adapted. *J. Exp. Biol.* **202**, 543–552.
- Rho, J. Y., Roy, M. E., Tsui, T. Y. and Pharr, G. M.** (1999a). Elastic properties of microstructural components of human bone measured by nanoindentation. *J. Biomed. Mater. Res.* **45**, 48–54.
- Rho, J. Y., Tsui, T. Y. and Pharr, G. M.** (1997). Elastic properties of human cortical and trabecular lamellar bone measured by nanoindentation. *Biomaterials* **18**, 1325–1330.
- Rho, J. Y., Zioupos, P., Currey, J. D. and Pharr, G. M.** (1999b). Variations in the individual thick lamellar properties within osteons by nanoindentation. *Bone* **25**, 295–300.
- Riggs, C. M., Lanyon, L. E. and Boyde, A.** (1993a). Functional associations between collagen fibre orientation and locomotor strain direction in cortical bone of the equine radius. *Anat. Embryol.* **187**, 231–238.
- Riggs, C. M., Vaughan, L. C., Evans, G. P., Lanyon, L. E. and Boyde, A.** (1993b). Mechanical implications of collagen fibre orientation in cortical bone of the equine radius. *Anat. Embryol.* **187**, 239–248.
- Rubin, C. T. and Lanyon, L. E.** (1982). Limb mechanics as a function of speed and gait: a study of functional strains in the radius and tibia of horse and dog. *J. Exp. Biol.* **101**, 187–211.
- Schryver, H. F.** (1978). Bending properties of cortical bone of the horse. *Am. J. Vet. Res.* **39**, 25–28.
- Ziv, V., Wagner, H. D. and Weiner, S.** (1996). Microstructure–microhardness relations in parallel-fibered and lamellar bone. *Bone* **18**, 417–428.